

# SUB-MILLIDEGREE-STABILITY AIR THERMAL CONTROL FOR A LARGE-VOLUME LITHOGRAPHY ENCLOSURE

Yong Zhao<sup>1</sup>, David L. Trumper<sup>2</sup>, Ralf K. Heilmann<sup>1</sup>, and Mark L. Schattenburg<sup>1</sup>

<sup>1</sup>Space Nanotechnology Laboratory, Massachusetts Institute of Technology, Cambridge, MA 02139

<sup>2</sup>Precision Motion Control Lab, Massachusetts Institute of Technology, Cambridge, MA 02139

## INTRODUCTIONS

The thermal control of environmental enclosures is becoming increasingly critical as precision metrology, lithography and machining systems require sub-nanometer tolerances. As shown in Table 1 & 2, the thermal control of  $\pm 5 \sim 50$  mK, which is typical for state-of-the-art equipment, will cause large errors on substrates. Some thermal control systems have achieved temperature stability of millidegrees or better using air-flow standard cell enclosures [1, 2] or enclosures utilizing flowing water as thermal control medium [3]. With large-volume air-flow enclosures, one-sigma air temperature stability of 2~3 mK at a single point has been demonstrated [4, 5]. In this paper we will report on how we improved the thermal control of an environmental enclosure designed for a precision lithography tool [5] to drive single-point one-sigma temperature stability down to sub-millidegree levels.

TABLE 1. Interferometer error caused by a change in the index of refraction of air inside the enclosure.

| The error of temperature control | Change in the index of refraction of air | Position error for 150 mm wafers | Position error for 300 mm wafers |
|----------------------------------|--|----------------------------------|----------------------------------|
| $\pm 50$ mK                      | 96.80 ppb                                | 14.5 nm                          | 29.0 nm                          |
| $\pm 5$ mK                       | 9.68 ppb                                 | 1.45 nm                          | 2.90 nm                          |
| $\pm 1$ mK                       | 1.94 ppb                                 | 0.29 nm                          | 0.58 nm                          |

TABLE 2. The error caused by the thermal expansion of the wafer chuck.

| The error of temperature control | Coefficient of thermal expansion (Super Invar) | Position error for 150 mm wafers | Position error for 300 mm wafers |
|----------------------------------|--|----------------------------------|----------------------------------|
| $\pm 50$ mK                      | 0.6 ppm/K                                      | 9.0 nm                           | 18.0 nm                          |
| $\pm 5$ mK                       |  | 0.90 nm                          | 1.80 nm                          |
| $\pm 1$ mK                       |  | 0.18 nm                          | 0.36 nm                          |

Our environmental enclosure, whose internal dimensions are approximately 1.8-m long X 1.5-m wide X 2.1-m high, consists of two identical air handler units [5]. As shown in Fig. 1,

in each unit the thermally well-controlled air flows into the chamber in the center and returns through the grills located at the top and bottom. The air returned through the top is cooled by a chiller coil and then reheated by electrical heaters to a controlled temperature. After mixing with the bottom return air, the reheated air is forced by a fan through an acoustic silencer to enter the chamber. The time for circulating the full chamber air is only 11 seconds. The thermal sensors in each unit for feedback thermal control are located in front of the central filter plane.

## MEASURING THE TRANSFER FUNCTION OF THE THERMAL SYSTEM

Measuring the transfer function of a system is one of the most critical requirements to achieve the desired performance. However, sometimes it is impossible to take a direct open-loop transfer function measurement because of noise issues or field-test limitations. Alternatively, calculating the transfer function based on the closed-loop frequency response measurement is utilized. As shown in Fig. 2, with an HP 35670A Dynamic Signal Analyzer, we inject a stimulus swept sine signal (**N**) into the loop and the frequency response measurement is taken at points **Y**<sub>1</sub> and **Y**<sub>2</sub>. The transfer function (**GTH**) of this thermal system is calculated from the measurement as below,

$$\left\{ \begin{array}{l} |GTH| = \left| \frac{Y_2}{Y_1} \right| / |G_c| \\ \Phi(GTH) = -180^\circ + \Phi\left(\frac{Y_2}{Y_1}\right) - \Phi(G_c) \end{array} \right.$$

A PI compensation controller,  $6\left(1 + \frac{1}{63s}\right)$ , is

utilized in the closed-loop frequency response measurement in order to make the thermal system perform around the desired temperature. Fig. 3 shows the closed-loop

frequency response measurement ( $Y_2/Y_1$ ). Due to the limit in minimal frequency for the swept sine signal, we can only make the frequency response measurement down to 0.015625 Hz. However, this is low enough for us to design the controller. The calculated open-loop transfer function (**GTH**) of the thermal system is shown in Fig. 4.

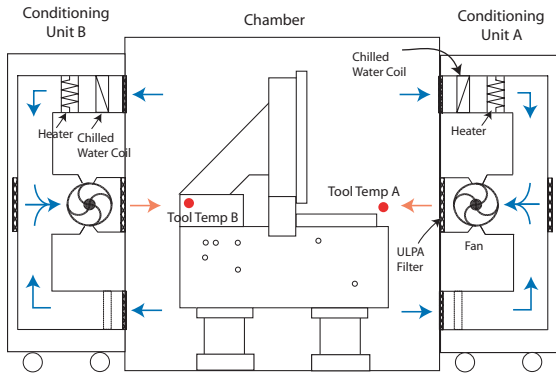


FIGURE 1. The environmental enclosure.

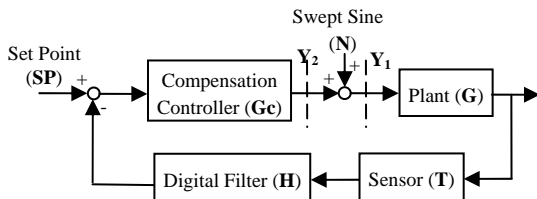


FIGURE 2. The diagram for measuring the transfer function of the thermal system.

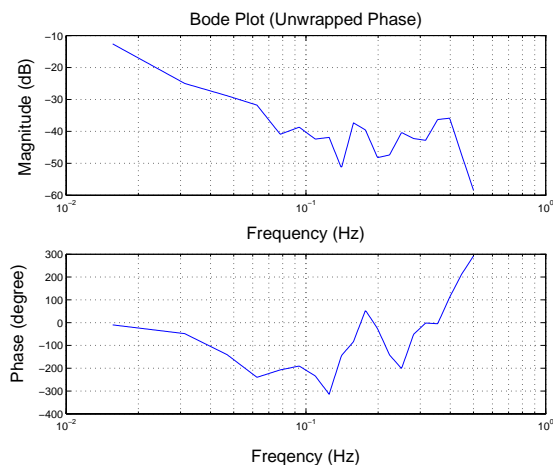


FIGURE 3. The closed-loop frequency response measurement ( $Y_2/Y_1$ ).

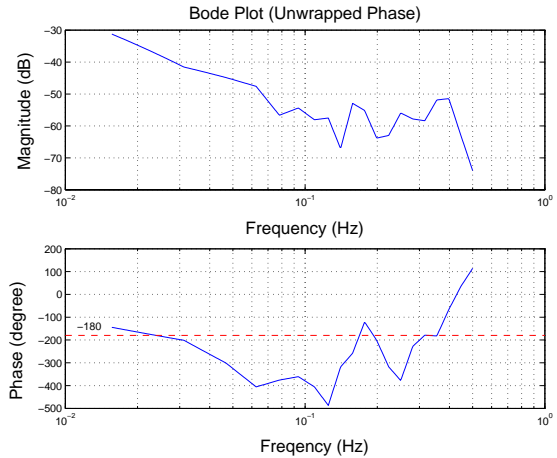


FIGURE 4. The calculated open-loop transfer function (**GTH**) of the thermal system.

### DESIGN A CONTROLLER FOR THE THERMAL SYSTEM

Based on the transfer function of the thermal system, we design a lead compensation controller ( $\frac{100s+1}{15s+1}$ ), which reduces the

overshoot by increasing the phase margin and a faster transient response is realized by increasing the gain crossover. The bode plots of the compensated system and uncompensated system are shown in Fig. 5.

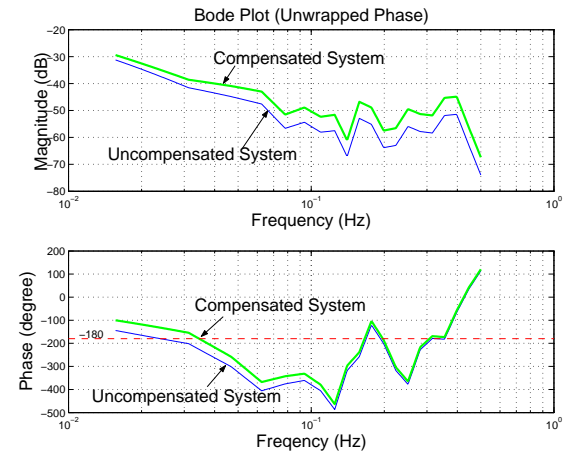


FIGURE 5. The bode plots of the compensated system and uncompensated system.

A PI controller ( $1 + \frac{1}{1000s}$ ) is also added into

the control system in order to eliminate the steady-state error. From Fig. 6, we find the steady-state error to be around 0.2 °C with respect to the set point (20 °C) when there is no

PI controller.

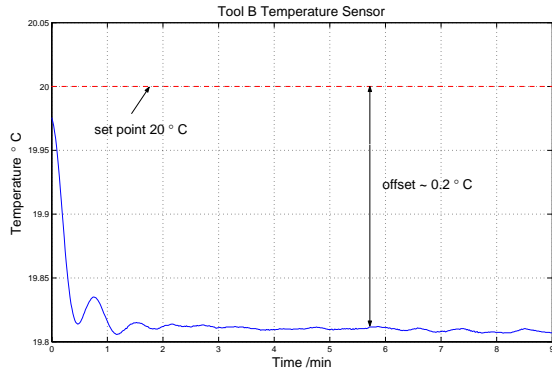


FIGURE 6. The performance of the thermal control system when there is no PI controller.

Figure 7 shows the diagram of our thermal control system. The controller is surrounded by a dashed line. An anti-windup block is utilized to avoid the effect of integrator windup [6]. Finally, we transformed our s-plane design to a digital implementation (z-domain).

### THE PERFORMANCE OF THE THERMAL CONTROL SYSTEM AND CONCLUSIONS

With the PI-lead compensation controller, one-sigma air temperature stability of less than 1 mK at a single point over 2 hours has been achieved, which is shown in Figs. 8 (a) and (b). The temperature sensor of the thermal system measured a one-sigma stability of 0.70 mK (Fig. 8 (a)). An independent temperature sensor measured one-sigma stability of 0.50 mK (Fig. 8 (c)), perhaps due to the resolution and the response time limitations of the sensor.

In this study, a method to measure the open-loop transfer function of a thermal system

has been developed. Based on the measured transfer function, a lead compensation controller together with a PI controller is designed for the thermal control of an environmental enclosure.

Sub-millidegree-stability air thermal control for a large-volume enclosure has been achieved.

### REFERENCES

1. D. Sarid and D. S. Cannell, "A  $\pm 15$  microdegree temperature controller", *Review of Scientific Instruments*, 45, 1082-1088 (1974).
2. J. Dratler, "A proportional thermostat with 10 microdegree stability", *Review of Scientific Instruments*, 45, 1435-1444 (1974).
3. H. Ogasawara, "Method of precision temperature control using flowing water", *Review of Scientific Instruments*, 57, 3048-3052 (1986).
4. K. M. Lawton and S. R. Patterson, "A high stability air temperature control system", *Precision Engineering*, 24, 174-182 (2000).
5. Paul T. Konkola, "Design and analysis of a scanning beam interference lithography system for patterning gratings with nanometer-level distortions", PhD dissertation, Massachusetts Institute of Technology, Department of Mechanical Engineering, June 2003.
6. Karl J. Astrom and Bjorn Wittenmark, "Computer-Controlled Systems: Theory and Design", Prentice Hall, 3rd edition (1996).

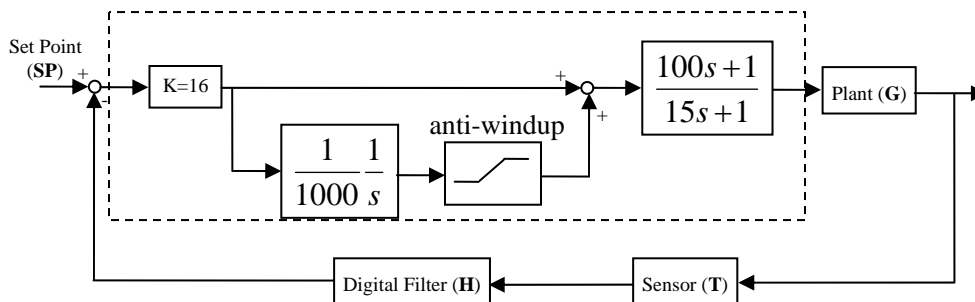


FIGURE 7. The diagram of the thermal control system. The part inside the dashed line is the controller.

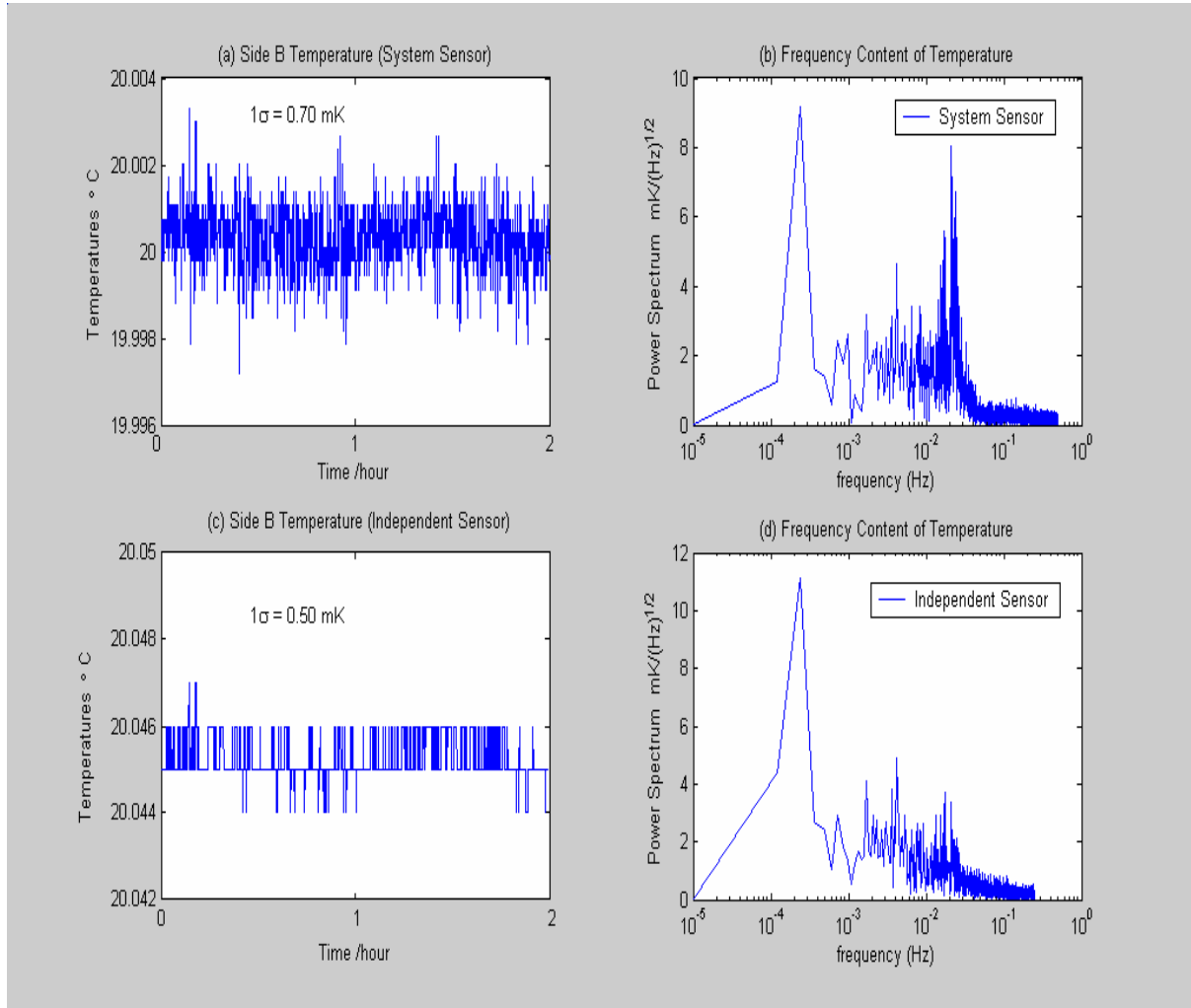


FIGURE 8. The diagram of the thermal control system. The part inside the dashed square is the controller.